THE ROLE OF FIBROBLAST GROWTH FACTOR SIGNALLING IN EPIMORPHIC REGENERATION

(Synopsis of thesis)

Isha Ranadive

DEPARTMENT OF ZOOLOGY, FACULTY OF SCIENCE,
THE MAHARAJA SAYAJIRAO UNIVERSITY OF BARODA,
VADODARA- 390002, INDIA

INTRODUCTION

Regeneration in an adult animal is a striking example of post-embryonic morphogenesis. It involves the recognition of tissue loss or injury, followed by mechanisms that reconstruct or restore the relevant structure (Brockes, 2001). There are three primary ways by which regeneration can occur. The first mechanism involves the dedifferentiation of adult structures to form an undifferentiated mass of cells that then becomes respecified. This type of regeneration is called epimorphosis and is characteristic of regenerating limbs. The second mechanism is called morphallaxis. Here, regeneration occurs through the re-patterning of existing tissues, and there is little new growth. Such regeneration is seen in hydras. The third type of regeneration is an intermediate type and can be thought of as compensatory regeneration. Here, the cells divide but maintain their differentiated functions. They produce cells similar to themselves and do not form a mass of undifferentiated tissue. This type of regeneration is characteristic of the mammalian liver (Gilbert 2014). A diagrammatic representation of these three types of regeneration has been portrayed in figure 1.

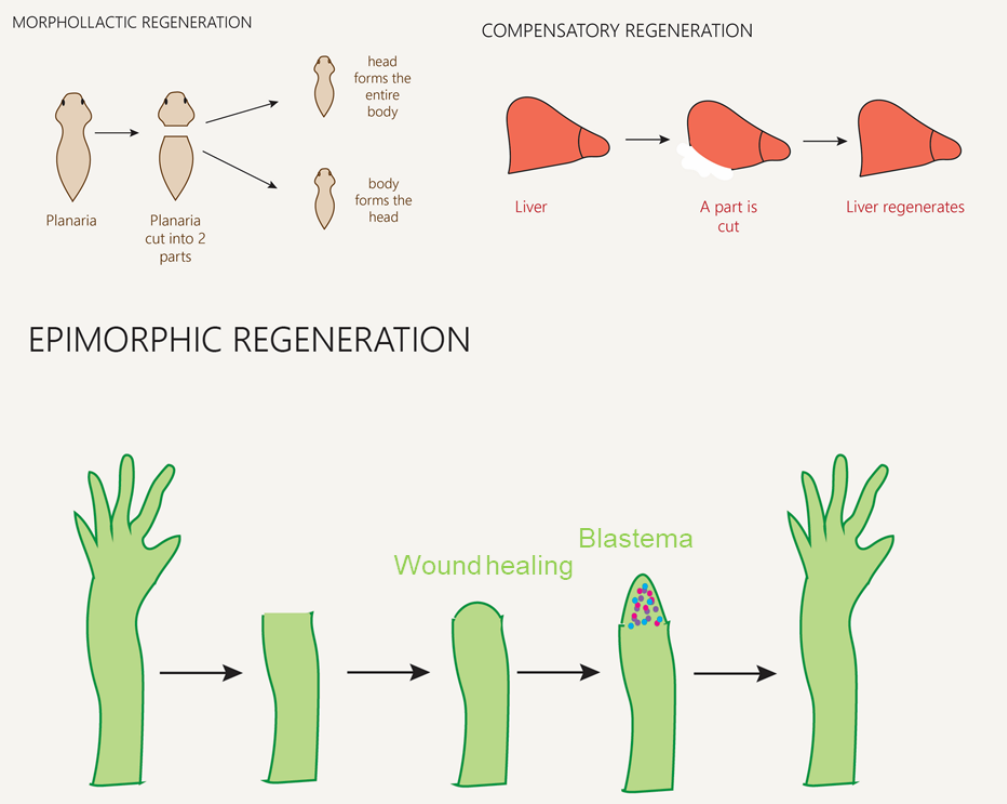

Figure 1: Types of regeneration

The ability of adult animals to regenerate large sections of the primary or secondary body axes is not found in all phyla. Six phyla, including rotifers and nematodes, are considered to exhibit cell constancy after embryological development (Hughes, 1989; S´anchez Alvarado, 2000). Out of these, our lab has been working on class reptilian wherein the model organism is *Hemidactylus flaviviridis* and class Pisces wherein the model organism is *Poecilia latipinna*. Lizards are the only amniotes endowed with the capacity to regenerate their lost tail through the process of epimorphosis. Unlike amphibians, lizards do not possess the power to regenerate its limb following an injury and hence making them the best candidate for studying wound healing patterns of both scar less and scarred healing. Further, wound healing, being an incredibly complex biological process with intricate molecular interaction amongst various cells at the site of injury, is modulated by the timed expression of a myriad of regulatory factors. Prominent among these factors are the members of epidermal growth factor (EGF), transforming growth factor beta (TGF-β), fibroblast growth factor (FGF), interleukin (IL) and tumour necrosis factor-α families (Penn *et al*., 2010; Makanae *et al*., 2016). In addition, vascular endothelial growth factor (VEGF), granulocyte macrophage colony stimulating factor (GM-CSF), platelet-derived growth factor (PDGF), connective tissue growth factor (CTGF) are known to influence the process of wound healing (Barrientos *et al*., 2008; Matsumoto *et al*., 2014).

The scarred wound healing is achieved through a multifaceted yet overlapping sequence of event namely hemostasis, inflammation, proliferation and remodelling at the site of injury. There are ample records to believe that these events are tightly regulated by several mediators that include, but not limited to, platelets (Sonneman and Bement, 2011), inflammatory cells (Grose *et al*., 2002), cytokines (Gillitzer and Goebeler, 2001), growth factors and matrix metalloproteinases (Madala *et al.*, 2012). A tissue when injured would immediately relay signals to the cells at the site of injury to form a provisional matrix over the wound to curtail blood loss. Immediately following hemostasis, the newly recruited platelet cells trigger a local surge of inflammation (Mutsaers *et al*., 1997). Once the inflammation subdues the proliferation phase begins wherein the wound is rebuilt with granulation tissue which is a collection of fibroblasts, inflammatory cells, and neovasculature wrapped in a matrix of collagen and extracellular matrix. In the subsequent maturation phase, the granulation tissue undergoes substantial remodeling with attended retraction of blood vessels to form an avascular structure called scar, a dense collagen tissue, that thoroughly covers the wound (Enoch and Harding, 2003; Sonneman and Bement, 2011).

Not surprisingly, even the scar-free wound healing begins with a hemostasis phase, however, after an acute hike early on, the inflammatory phase is suddenly truncated, which is where the scar-free healing swerves away from that of the scarred one. This abrupt drop in the inflammation marks the beginning of proliferation that allows the epidermal cells to rapidly divide and migrate as a layer to cover the wound surface which eventually stratifies to form a multi-layered apical epithelial cap (AEC). The AEC, like an embryonic organizer, sends regulatory signals to the underlying mesenchyme and the latter responds by recruiting a pool of blastemal cells which proliferate and later get re-specified to recreate the lost tissue (Carlson 1970). The various phases of scarred and scar-free wound healing are depicted in figure 2.

Further, wound healing, being an incredibly complex biological process with intricate molecular interaction amongst various cells at the site of injury, is modulated by the timed expression of a myriad of regulatory factors. Important among these factors are the members of epidermal growth factor (EGF), transforming growth factor beta (TGF-β), fibroblast growth factor (FGF), interleukin (IL) and tumor necrosis factor-α families (Penn *et al*., 2012; Makanae *et al*., 2016). In addition, vascular endothelial growth factor (VEGF), granulocyte macrophage colony stimulating factor (GM-CSF), platelet-derived growth factor (PDGF), connective tissue growth factor (CTGF) are known to influence the process of wound healing (Barrientos *et al*., 2008; Matsumoto *et al*., 2014). FGF has multiple roles in the process of development which are listed below in table 1, however very few have been identified to play a role in the process of regeneration and wound healing. From work done in the lab and other current studies, FGF was chosen so as to elucidate its role in epimorphic regeneration as well as in the scarred wound healing. Moreover, a temporal expression screening of these molecules is yet to be attempted in the appendages of lizard during the course of wound healing. Hence, it was thought pertinent to compare their expression pattern during the course of scarred as well as scar-free wound healing in the limb and the tail respectively of lizard Hemidactylus flaviviridis.

Table 1: Role of FGFs in different developmental processes

Ligand	**Role**
FGF1	Endothelial cell proliferation and angiogenesis
FGF2	Endothelial cell proliferation and hematopoesis
FGF3	Chondrogenesis and negative regulator of bone growth factor during ossification
FGF4	Formation of AER, mesenchyme proliferation, angiogenesis and neurogenesis
FGF5	Cell proliferation and differentiation
FGF6	Embryogenesis

FGF7	Regulator of liver progenitor cells
FGF8	Cell growth, morphogenesis, and tissue repair
FGF9	The proliferation of mesenchymal cells
FGF10	Formation of AER
FGF11	No specific function
FGF12	No specific function
FGF13	Neural development
FGF14	Voltage-gated sodium channels activity in the neuron
FGF15	Neurogenesis and opposes FGF8
FGF16	Embryonic heart development
FGF17	Embryonic development
FGF18	Chondrogenesis and osteogenesis

(Ollendorff, 1993; del Moral, 2006)

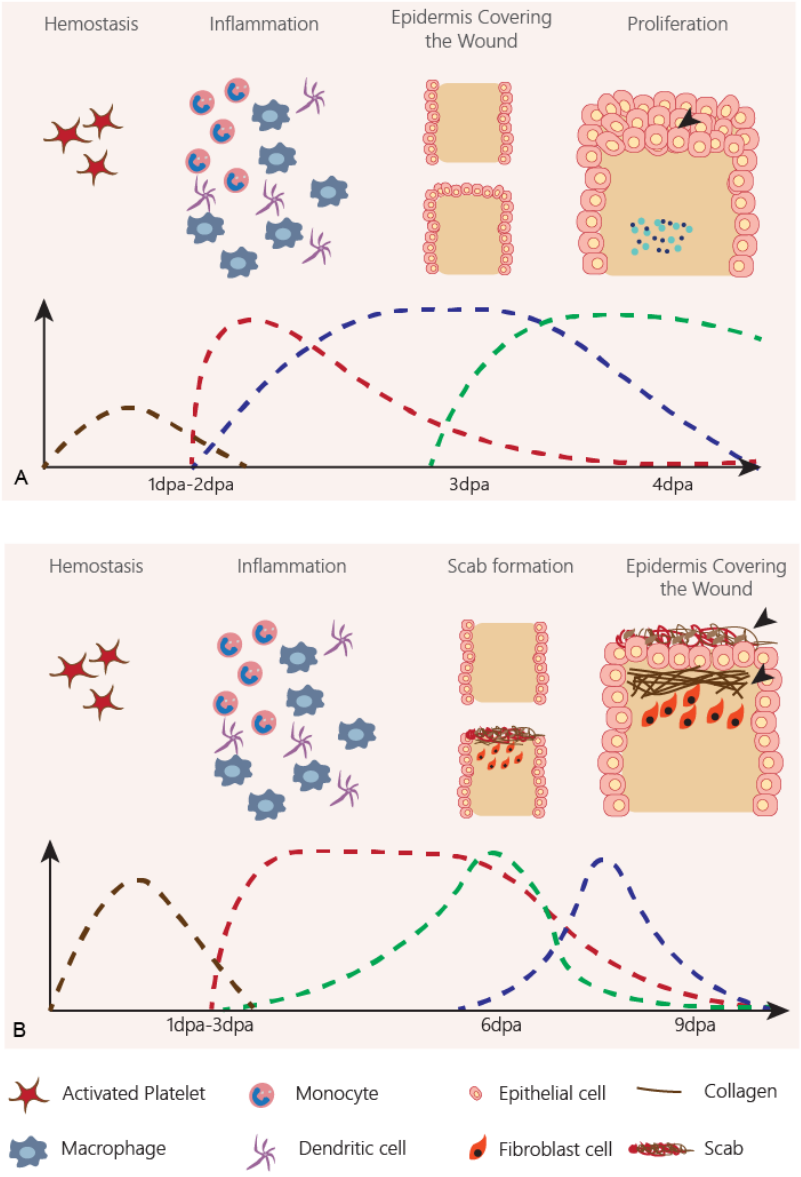

Figure 2: Phases in wound healing.

A) Depicts the scar-free wound healing where the epidermis covers the wound and then proliferates to form the Apical epithelial cap (AEC) as shown by the arrowhead. B) Shows the scarred wound healing where re-epithelialization starts along with fibroblast proliferation, deposition of collagen (shown by arrowheads) and ECM development to form the granulation tissue. Brown dotted line represents the hemostasis phase, red dotted line shows the inflammation phase, blue dotted line is for epidermis covering the wound and green dotted line depicts the proliferation of epidermis in scar-free wound healing while in scarred wound healing it represents proliferation of fibroblast cells and scab formation.

OBJECTIVE

To elucidate the role of FGF in cellular processes which drive the appendage to undergo either regeneration or scar formation when subjected to injury.

- Screening of FGFs for its temporal expression in regenerating and the non-regenerating appendage of lizard.
- Finding out the variation in cellular processes like proliferation, apoptosis, and angiogenesis in scar-free and scarred wound healing in lizards tail and limb following amputation.
- Studying the role of FGF in EMT and how EMT drives the process of regeneration in lizards tail which is entirely absent in scarred wound healing in the lizard limb.

MATERIALS AND METHODS

Animal Maintenance:

Healthy adult northern house geckos of either sex having average snout to vent length of 10cm were chosen for the study. They were acclimatized for a week and maintained all through the experiment in well ventilated wooden cages. The cages were housed in a room at a controlled temperature of 36±2°C and 40-70% relative humidity. The photoperiod was kept at 12:12 hours of light: dark. Lizards were fed with cockroach nymphs daily, and water was given ad libitum. Autotomy was induced in the tail by applying mild pressure with a foot ruler on the 3rd segment from the vent. The limb was amputated under hypothermia. The animal was placed on a pre-cooled tile, and the ice pack was applied to the limb to be amputated. With a sharp, sterile surgical blade, the forelimb of the lizard was amputated. The experimental protocol (MSU-Z/IAEC/15-2017) was approved by the Institutional Animal Ethics Committee (IAEC), and all the experiments were performed as per the guidelines of Committee for the Purpose of Control and Supervision of Experiments on Animals (CPCSEA), India.

Experimental design

The tissue samples were harvested in a sterile condition at the selected time interval. Time points for tissue collection were decided based on the discrete events associated with wound healing in the tail and in the limb. These have been characterized for the tail through the course

of various studies in our lab (Buch *et* al., 2017; Murawala *et al.,* 2017). It has been observed through histology in our lab that the following autotomy, hemostasis is achieved rapidly and a scab is formed as early as 1dpa. Subsequently, a thin layer of epithelium covers the wound surface on 2dpa. Thereafter, the epithelium continues to proliferate and stratifies into a multi-layered AEC that displaces the scab on 4dpa. Hence the time points selected for tissue collection were 0dpa (representing uncut resting stage), 1dpa, 2dpa, 3dpa and 4dpa.

On the other hand, wound healing in the amputated limb is achieved only on 9dpa in the selected housing condition. Based on a continuous morphological observation on a severed limb and taking reference from (Alibardi, 2010; Vitulo *et al.,* 2017), the events occurring therein were found to be different from that of the tail. Hemostasis phase in case of an amputated limb is longer compared to tail. Therefore, even on 3dpa, the cut end of limb shows only a scab with no epithelial layer beneath it. On 6dpa, limb displays a thick blood clot and is in granulation phase. Proper scarring is, however, achieved on 9dpa. Hence, the time points selected for limb were 0dpa (representing uncut resting stage), 3dpa, 6dpa, and 9dpa. The study was composed of nine groups in total; five groups in case of the tail and four groups for limb tissues. Each group consisted of six lizards for individual experiments. The tissues were processed as per the requirement described in the following sections.

Histology

Histology was performed for tail tissues at 0dpa, 2dpa, and 4dpa and at 0dpa, 3dpa and 9dpa for limb tissues. The tissues were stored in 10% neutral buffered formalin and decalcified by EDTA, followed by dehydration and embedding into paraffin blocks. Sections were cut at a thickness of 7µm and stained with Harris' hematoxylin and eosin. The stained samples were observed under Leica DM2500 research microscope, and the representative digital images were grabbed using Leica EC3 camera. The microscopic measurements of various tissues in the tissue sections were done using LAS EZ software.

2D-Gel electrophoresis

To get a complete protein profile of the tail and limb in their resting stage and also after amputation when the wound gets healed, a 2DGE was carried out. The protein load was kept

at 50µg/strip. A broad range study was done, and thus the strip used was of pH3 to pH10 of 7cm. The program set was:

Steps	Voltage	Mode	Time	Unit
1	250	Rapid	00:15	HH:MM
2	4000	Gradual	01:00	HH:MM
3	4000	Rapid	15000	Volt-hour
4	500		HOLD	

The first dimension separation was carried out in a PROTEAN® i12™, followed by SDS-PAGE. The gels were stained by silver staining method. Analysis of the spots was done by using the PDQuest 2-D analysis software, version 8.0.

Immunohistochemistry

For immunolabelling, longitudinal cryosections (8-10µm) were cut from freshly collected tissues, fixed in acetone at -20ºC for 15-20 minutes and air dried for 15 minutes. Sections were then rehydrated with PBST (Phosphate Buffered Saline with 0.025% Tween-20) followed by blocking with corresponding normal serum [Genei, Merck, USA; 10% in PBS with 0.5% Bovine serum albumin (PBS-BSA)] for 1hour at room temperature (RT). Sections were then incubated with Anti-FGF2 IgG rabbit (Sigma-Aldrich, USA, 0.5µg/ml). For primary antibody, FITC-conjugated secondary antibody (Sigma Aldrich USA, 0.1µg/ml) was used, and the expression was observed under a fluorescent microscope. The representative images were captured using a digital camera (Leica, EC3) mounted on the Leica DM2500 microscope.

BrdU labeling

Intraperitoneal injection of BrdU (Sigma Aldrich, USA) at a dose of 100mg/kg body weight was given to the animals at 3dpa, and tail tissue was harvested at 4dpa by inducing autotomy. In the case of the limb, BrdU was administered on 8dpa and tissue was collected for sectioning on 9dpa. Tissues were embedded in cryo-embedding medium (Sakura Finetek, Japan) and fresh frozen sections (8-10µm) were taken on 0.01% poly-L-lysine coated slides. The sections were fixed in cold acetone (15-20min at -20ºC) and air dried for 15minutes followed by treatment with 2N HCl for 30-60min at 37°C. Sections were blocked using a normal serum (10% in PBS-BSA) for 1hour at RT and incubated with 1:100 dilution of Mouse Anti-BrdU (Sigma-Aldrich,

USA) in PBS. Sections were then incubated with 1:50 dilution of Goat Anti-Mouse IgG-FITC (Genei, Merck, USA) in PBS for 2 hours at RT, washed, mounted with PBS: glycerol (1:1) and observed under a fluorescence microscope (Leica DM2500 utilizing LAS EZ software).

Acridine orange and Ethidium Bromide staining

Cold sections (7µm) were taken using cryotome (Reichert-Jung Cryocut E, USA) for wound epithelium stage in the tail at 4dpa and scarring in the limb at 9dpa. The sections were washed with phosphate buffer of pH 7.4 (10mM PO_4^{3-}, 137mM NaCl, and 2.7mM KCl) thrice. Following washing, AO/EtBr stain (100µg/ml) was added for 10sec, and the sections were immediately washed with phosphate buffer. All the images were taken under a fluorescent microscope (Leica DM2500 utilizing LAS EZ software).

Western Blot

Tissues were harvested from all the nine groups and homogenized in lysis buffer (50mM Tris pH 7.5, 200mM NaCl, 10mM $CaCl_2$ and 1% Triton-X 100) containing a protease inhibitor. The samples were centrifuged at 12000rpm for 10min, and protein estimation was done using the Bradford method (1976). 40µg of the protein of each sample was loaded and separated on a 12% SDS-PAGE. These proteins were transferred onto PVDF membrane through semi-dry transfer method by applying 100mA for 25min. The primary antibodies used to probe each protein of interest were Anti-Fibroblast growth factor 2 IgG rabbit (Sigma Aldrich USA, 0.1µg/ml), Anti-Fibroblast growth factor receptor 1 IgG rabbit (Sigma Aldrich USA, 0.1µg/ml), Anti-Fibroblast growth factor receptor 3 IgG rabbit (Sigma Aldrich USA, 0.1µg/ml), and Anti- β-actin IgG mouse (Santa Cruz Biotechnology USA, 0.01µg/ml). The blot was developed by using the ALP, BCIP-NBT system (Sigma Aldrich, USA).

Quantitative Real-Time PCR

Total RNA was isolated from the limb and tail tissue homogenates using TRIzol reagent (Applied Biosystems, USA). One microgram of total RNA was reverse-transcribed to cDNA using a one-step cDNA Synthesis Kit (Applied Biosystems, USA). Primers were designed using PrimerBlast tool of NCBI, details of which are given in table 2. Quantitative real-time

PCR was performed on a Light Cycler 96 (Roche Diagnostics, Switzerland) with the following program: 3 min at 95ºC as initial denaturation step and 45 cycles with each cycle of 10s at 95ºC, 10s at 60ºC and 10s at 72ºC). Gel electrophoresis and melt curve analysis were used to confirm specific product formation. 18SrRNA was taken as endogenous control. The fold change was computed using the method of Livak and Schmittgen (2001). In order to minimize variations among biological individuals, the tissue samples from six lizards were pooled and for each variable analyzed in RT-PCR three technical replicates were performed to reduce the experimental error.

Table 2: Primer sequence obtained from NCBI

Gene	Forward primer	Reverse primer
fgf1	ACTCTCCGGAAAAGAAACCTTG	GTGGGTTTCTGGTCCCTTCA
fgf2	ATCCGGGAGAAAAACGACCC	TTGGTCGTCTCGCTCCAAAC
fgf4	GCACCTGACCACAGGTATCC	GGCCCAGAGCAAAACATTGG
fgf8	GAGACCGACACCTTTGGGAG	TTGCCGTTACTCTTGCCGAT
fgf10	GTGCGGAGCTACAATCACCT	TCCAATATGCTGAAGGGGCA
fgf12	ACCGCCAAGACAACGATGAT	CATTTCCAAGCAAGCCCCTC
fgf16	ACAAGGCGAACGTCACAGAT	TACGTCCCGAGCCTACTGAA
fgf17	CATGCCACTTTTGGGAAGCC	ACGAGTGATTCTCCCCCTGA
fgf20	GATTCTGGGCGGCGATACTT	TCAGCTGTATCCCAGCACATC
fgf21	GAACTCACAACACGGCGTTC	CGAGTCCAGGTTGAAGTCCC
fgf22	ACACTCATCCATTTGGACTAAACTC	GACACAGATCCTTCCGGTGC
fgfr1	CCGTCCAGCAACACCTACTT	TGAGTCCACAGACACTGTTACC
fgfr2	GGGTTCAGCAAAGGTGCAAG	TTTGGGGTCAGGTATGCGAC
fgfr3	CGCCGACATCCTCATCTACC	GCTGTCTCTTGAGGGGGAAC
tgfβ1	CATGGCGAACAGGAACAACAGC	AGTGGTGAGCAGCTGGAAATTG
tgfβ2	AACCACAGAGCTGCCACTTG	CTTGGTGGGATGGCATTTTCG
tgfβRI	AGGGACACAAGGAAAACCAGC	GGAGTCATGTCGAACAGCCA
tgfβRII	ACTGGTGTTCGTTTCCACAGC	ATCACCACGGCAACCAAGAC
p53	CAGCCAAGTCTGTGACTTGCACGTAC	CTATGTCGAAAAGTGCTTCTGTCATC
p21	CTGGAGACTCTCAGGGTCGAA	CCAGGACTGCAGGCTTCCT
bcl2	ATGTGTGTGGAGAGCGTCAACC	GCATCCCAGCCTCCGTTATC
Bax	CCTTTTCTACTTTGCCAGCAAAC	GAGGCCGTCCCAACCAC
Bad	CTTTAAGAAGGGACTTCCTCGC	GTGGAGTTTCGGGATGTGGA
cytC	GAACAAAGGCATCATCTGGGG	GGCAGTGGCCAATTATTACTCA
Cl.caspase 3	AAAGATGGACCACGCTCAGG	TGACAGTCCGGTATCTCGGT
PCNA	TGTTCCTCTCGTTGTGGAGT	TCCCAGTGCAGTTAAGAGCC

RESULTS:

Morphology and Histology

Lizards, as a taxonomic group, are more closely related to mammals than are the urodeles. They are also endowed with well-structured appendages to aid their terrestrial mode of life much akin to their mammalian counterparts. In the current study, the healing pattern in two different appendages, viz., tail and limb, was assessed by observing the histological status of both, post-amputation and also during various stages of wound healing. Autotomy, when induced in the tail, leads to exposure of a variety of tissues like muscles and adipose along with the vertebral column (Figure 3A and 3B). However, in the amputated limbs, in addition to the soft tissues mentioned earlier, humerus bone too was vividly seen in the histological section (Figure 4A and 4B). Tail, being the fat storage organ of the lizard, exhibited thick layers of adipose tissue (Figure 3B and 3D), when compared to the limb (Figure 4C and 4D). As the bone can be seen protruding out from the limb (Figure 4A and 4B), in tail the two lateral processes protrude conspicuously (Figure 3C). After 2dpa in the tail, a proliferating epithelium covered the wound, as revealed in Figure 3E and 3F with an average thickness of 44.65µm (Figure 3G and Table 3). Later at 4dpa (Figure 3H and 3I) which is the WE stage, a more thickened epidermis of 91.93µm ($p \leq 0.001$) was observed (Figure 3J and Table 3). However, on the lateral sides of the tail, the thickness of the epithelium was 12.52µm (Figure 2K and Table 3). On the contrary when the amputated limb was monitored at 3dpa, no epithelial layer was visible at the wound surface (Figure 4E and 4F), instead blood clot was seen to cover the open bone surface (Figure 4G). At 9dpa, i.e., in the scarred limb tissue, a fully covered and healed structure was displayed, which differs significantly from the previously described completely healed tail (4dpa). Along with epithelium, dense connective tissue was observed over the wound surface (Figure 4H, 4I and 4J). On the lateral side, the mean thickness of connective tissue was 193.99µm (Figure 4K and Table 4), while immediately over the wound it was 369.15µm which was significantly high ($p \leq 0.001$) (Figure 4L and Table 4). However, the newly formed epithelial layer was just 12µm thick which is the standard thickness witnessed in the resting skin of the limb and tail of the lizard (Figure 4C and Table 4).

2D Gel electrophoresis

Since the focus of this study was to identify proteins that were either positively or negatively correlated with the tail regeneration process as well as during the scarring of the limb in H. flaviviridis, protein extract was run on a 7cm IPG strip followed by separating the proteins further on SDS-PAGE gels. Two-dimensional gels of wound healing stages (1dpa, 2dpa, 3dpa and 4dpa), when compared to the resting stage (0dpa) of lizard H. flaviviridis tail and wound healing stages of scarring limb (3dpa, 6dpa and 9dpa) when compared to resting stage (0dpa) showed differentially expressed peptides. Computational analysis of these 2-D gel images with PDQuest software revealed a number of spots. In the resting stage, a total number of 487 protein spots were present, while in 1dpa, 2dpa. 3dpa and 4dpa of tail 389, 385, 412 and 485 were recognized. In case of limb, the resting tissue revealed 471 spots while 3dpa, 6dpa and 9dpa revealed 315, 367 and 469 spots. By using the software, a Venn diagram was generated which depicts the number of spots which are commonly present within the stages as well the spots which are newly expressed in the specific stage of tail and limb wound healing (figure 5)

Following the analysis by PDQuest software version 8.0, a number of spots were sequenced, and multiple fibroblast growth factors were differentially expressed in both the healing stages of tail and limb which lead to further screening of remaining fgfs (Table 4). Based on this result, we chose the FGF signalling pathway and many other down-stream regulators which are required for fgfs to regulate the processes like proliferation, apoptosis, angiogenesis, cell migration and epithelial to mesenchymal cell transition. All these processes play a crucial role in the regeneration of tail and scarring of the limb on injury or amputation.

Gene expression study for screening fgf transcripts

Members of FGF family have been known since long to induce and sustain cell proliferation, angiogenesis and also in cell migration at the site of amputation. Hence, their expression level was studied at the mRNA level during the wound healing phase of the tail as well as a limb in a lizard (Figure 6A and 6B). A steady increase in the mRNA levels of *fgf1*, *fgf2, fgf8*, and *fgf12, fgf16, fgf17, fgf20, fgf21* and *fgf22* was observed in regenerating tail as healing progressed from 0 dpa to 4 dpa (Figure 6A). However, when the expression levels in all the stages were compared to that of resting stage, i.e., 0dpa, a sharp increase of 50-fold change was noticed for *fgf10* on 3dpa unlike the other fgfs screened (Figure 6A). In tandem with the rise in *fgfs*, *fgfr1, fgfr2* and *fgfr3* were also found elevated from 1dpa to 4dpa (Figure 6A). However, the limb

healing stages which are 0, 3, 6 and 9dpa showed a different trend to that observed in the tail. There was an increase in transcripts of *fgf1*, *fgf2*, *fgf8* and *fgf10* at 3dpa but a sharp decline was seen in subsequent stages (Figure 6B). *fgf4*, *fgf12*, *fgf20*, *fgf21*, *fgf22* were down-regulated till 9dpa which also coincided with the levels of receptor *fgfr1*, *fgfr2* and *fgfr3*. However, *fgf16* after 3dpa shot up at 6dpa and then was subdued in next 3days (Figure 6B).

Western Blot analysis

In order to reaffirm the result obtained from qRT-PCR, western blot of FGF2, FGFRI and FGFRIII were performed. FGF2 showed a steady increase from 0doa to 4dpa in case of tail wound healing (Figure 7A) while in limb a down-regulation of this protein was observed on 3 and 6dpa which increased later on at 9dpa after the completion of collagen deposition at the site of injury (Figure 7B). FGFRI showed a decrease on 1dpa and 2dpa but the levels were significantly elevated at 3dpa and 4dpa in tail (Figure 7A) while in limb a steady decrease was observed from 0dpa to 9dpa subsequently (Figure 7B). FGFRIII showed low level in 0dpa and 1dpa in tail but these levels hiked from 2dpa till 4dpa (Figure 7A), however in case of limb again a steady decrease was observed (Figure 7B).

Immunohistochemistry of FGF2, FGFRI and FGFRIII

After performing the western blot analysis, FGF2 was localised in the healing tissue of tail and limb. The results obtained showed apical epithelium cap and the underlying tissue to be positively stained for FGF2 profusely in the tail at 4dpa (Figure 8A), however their expression was restricted to the epithelium in case of limb at 9dpa and showed no immuno-staining in the underlying scarred tissue (Figure 8B).

BrdU incorporation in the healing tail and limb followed by gene expression of pcna

As FGFs have a prominent role in the process of proliferation, BrdU incorporation was performed to check whether up-regulation of fgfs is actually playing a role in the process or not. BrdU labelling revealed the presence of proliferating epidermis and a pool of dividing cells underneath (Figure 9A). Quite contrary to the observations in the tail tissue at wound epithelium stage (4dpa), only faint BrdU was observed in the scarred limb epithelium (9dpa)

indicating only basal levels of proliferation at a corresponding stage in the limb (Figure 9B). Furthermore, to find the actual trend of proliferation across the stages of wound healing, pcna at transcript level was studied and a steady increase was seen during tail wound healing stages with a 100-fold increase at 4dpa, as compared to 0dpa (Figure 9C). The healing limb also showed a progressive increase in pcna level but the fold change observed at 9dpa was just 10-fold (Figure 9D).

Acridine orange and ethidium bromide staining followed by gene expression of apoptotic markers

To further validate the results of BrdU incorporation, AO/EtBr staining was performed for examining the tissues undergoing proliferation and apoptosis. AO/EtBr staining was done on fresh frozen sections of 0dpa and 4dpa tail tissue along with 0dpa and 9dpa tissues of the healing limb. Both, the tail and limb tissues at 0dpa revealed live cells emitting green signal (Figure 10A and 10B). By 4dpa, in tail, a proliferating epidermis characterized by green fluorescence was predominantly observed along with few pro-apoptotic cells stained yellow (Figure 10C and 10E). On the contrary the limb tissue on 9dpa revealed heightened apoptosis marked by orange nuclear EtBr staining at the site of injury (Figure 10D and 10F). It is well perceived that immediately following injury the wound surface induces apoptosis to clear out the debris and in the subsequent phase of wound healing, regulated apoptosis facilitates a balanced proliferation and hence, transcript levels of caspase3, bax, bad, cytC, p53, p23 and bcl2 were quantified by real time PCR in the tissues collected from tail and limb during wound healing. On amputation of tail, within 1dpa, a 2-fold increase in caspase3 was observed which remained persistent till 2dpa (Figure 10G). Nevertheless, caspase3 returned to its basal levels at 3 and 4dpa (Figure 10G). All the other apoptotic genes studied namely, bax, bad, cytC, p53 and p23 remained down-regulated all through the healing stages of the tail (Figure 10G). However, in order to gain further insight into the regulation of apoptosis, expression pattern of anti-apoptotic gene bcl2 was ascertained and it was observed that the transcript levels of bcl2 remained subdued at the initial stages of healing tail, followed by an elevated expression at 3 and 4dpa, the observations being an exact contradiction to observed levels of caspase3 (Figure 10G). On the other hand, in the limb healing stages, except for bad, all the other genes remained down-regulated at 3dpa and 6dpa (Figure 10H). At 9dpa a sudden increase in these levels was noted, while in the same time frame, bcl2 showed an opposite trend in limb to that of the tail,

as higher levels were found at 3dpa and 6dpa, which subsequently declined at 9dpa (Figure 10H). Apart from the major genes involved in apoptosis, tgf-β levels were also screened as they have an important role in mediating apoptosis and wound healing. Both, tgf-β1 and tgf-β2 levels did not change significantly during the wound healing phase of the tail, but the scarring limb showed distinctly elevated expression of the same molecules, when compared to the resting tissue (Figure 10I). On the contrary, expression of tgf-β3 showed an increasing trend in the tail from 1 to 4dpa (Figure 10I) while its levels were found down-regulated in limb from 3dpa to 9dpa (Figure 10J). Along with the ligands, tgf-β receptors were also screened and tgf-βRI was found to be up-regulated at 9dpa in limb (Figure 10J) and down-regulated in the tail from 1dpa to 4dpa respectively (Figure 10I). tgf-βRII had a 2-fold increase in the tail from 1dpa to 4dpa (Figure 10I) but in limb no significant change was observed (Figure 10J).

Tissue layers analyzed	Thickness in µm
Lateral Epithelium (Normal resting stage)	12.52 ± 0.91
Epithelium Covering Wound at 2dpa	44.65 ± 1.28***
Epithelium Covering Wound at 4dpa	91.93 ± 3.89***,###

Table 3: Thickness of epithelium (in µm) during different stages of wound healing in tail.

Values are expressed as mean ± SEM. Thickness of epithelium at 2 and 4dpa was compared with the thickness lateral epithelium using One-way ANOVA followed by Bonferroni's Multiple Comparison Test, represented by asterisk. *** represents $p \leq 0.001$. Wound epithelium thicknesses of 2dpa and 4dpa were also compared with each other using the same test denoted by hash. ### represents $p \leq 0.001$, n=6.

Tissue layers analyzed	Thickness in µm
Lateral Connective tissue (Normal resting stage)	107.5 ± 4.51
Connective tissue at Wound site at 9dpa	369.15 ± 21.79***
Lateral Epithelium (Normal resting stage)	17.75 ± 3.87
Epithelium Covering Wound at 9dpa	12.78 ± 0.71

Table 4: Thickness of epithelium and connective tissue (in µm) during different stages of wound healing in limb.

Values are expressed as mean ± SEM. Thickness of connective tissue at wound site was compared with that of the lateral side using Unpaired t-test denoted by asterisk. *** represents $p \leq 0.001$, n=6. The epithelium thicknesses of 9dpa and lateral side were compared using Unpaired t-test which was found to be non-significant.

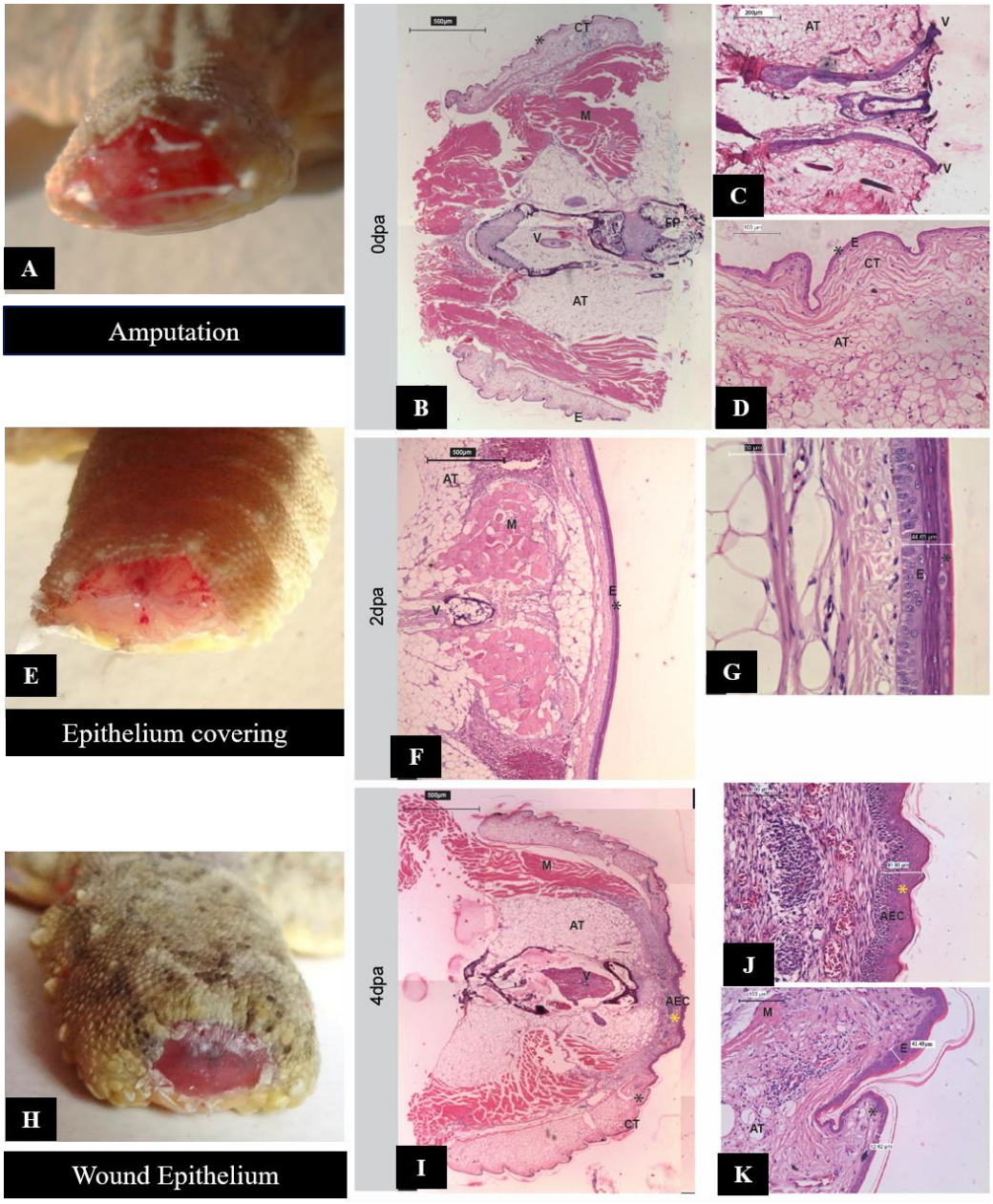

Figure 3: Histology of Tail and its wound healing stages. A) Picture of tail on amputation; B) Longitudinal section of tail showing fracture plane (FP), muscles (M), adipose tissue (AT), epithelium (E) and connective tissue (CT); C) Magnified image of resting tail showing the vertebral column processes (V) projecting out; D) Magnified image showing arrangement of E, CT and AT; E) Picture of tail on 2dpa reveals a smooth surface of epithelium covering the wound; F) Epidermis covering the wound surface at 2dpa and G) The thickness of epithelium formed is 44.65µm; H) Picture of tail on 4dpa shows a proper covering of epithelium over the wound surface called as apical epithelial cap; I) At 4dpa, wound epithelium formation occurs that is depicted by proliferating epidermis also called as apical epithelial cap (AEC); (J) shows the magnified image of AEC by arrow which has a thickness of 91.93µm; K) This section clearly shows that lateral epidermis maintains its thickness at 12.62µm whereas the epidermis moving towards the AEC has a thickness of 41.49µm. '*' represents the area that has been shown in the magnified image. All the sections are longitudinal in orientation and stained with hematoxylin eosin. Magnification for A, D and F is 40X, B is 100X, C, G and H is 200X and E is 400X, n=6.

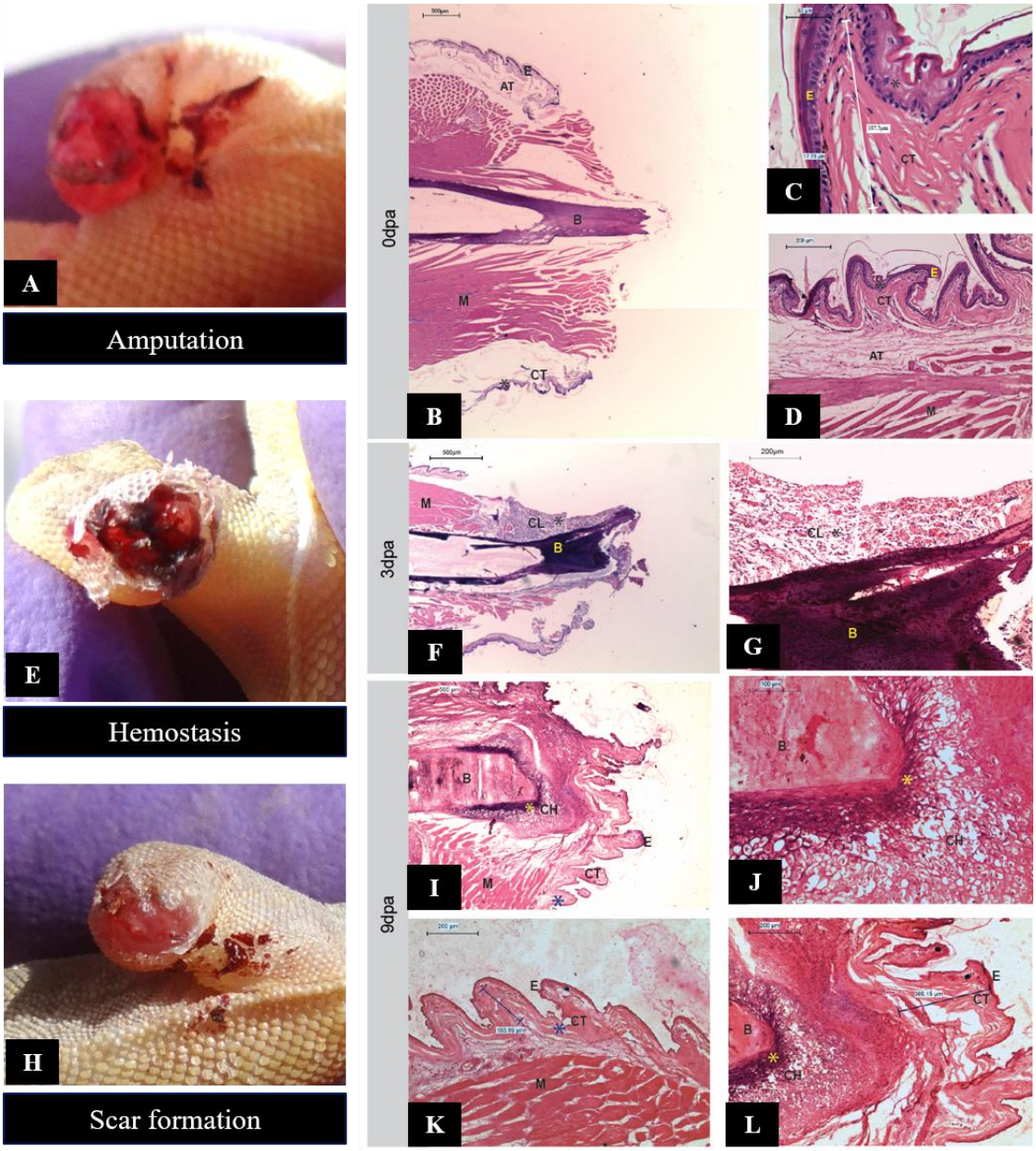

Figure 4: Histology of Limb and its wound healing stages. A) Morphology of limb on 0dpa shows bone protrusion, blood oozing out; B) Histology of limb, shows exposed tissues like muscles (M), connective tissues (CT), humerus bone (B), epithelium (E) and adipose tissue (AT); C) Enlarged image showing connective tissue with a thickness of 107.5µm and epithelium having same thickness as that of tail which is 17.75µm; D) Arrangement of tissues can be observed which is similar to that of tail except AT being thicker in tail and CT being comparatively thicker in limb; E)Picture of limb on 3dpa is showing a blood clot F) displays histology of limb at 3dpa with no epithelium covering and G) represents persistent blood clot over the bone; H) Picture of limb showing smooth healed surface; I) shows the healed limb wherein connective tissue (CT) can be observed covering the wound surface; J) depicts the chondrocytes which replace the clot over the humerus bone; K) shows lateral connective tissue with no difference in thickness from that of resting limb whereas in L) just at the wound site the thickness of connective tissue in 369.15µm. '*' represents the area that has been shown in the magnified image. All the sections are longitudinal in orientation and stained with hematoxylin eosin. Magnification for A, D and F is 40X, C, E, H, and I are 100X, G is 200X and B is 400X, n=6.

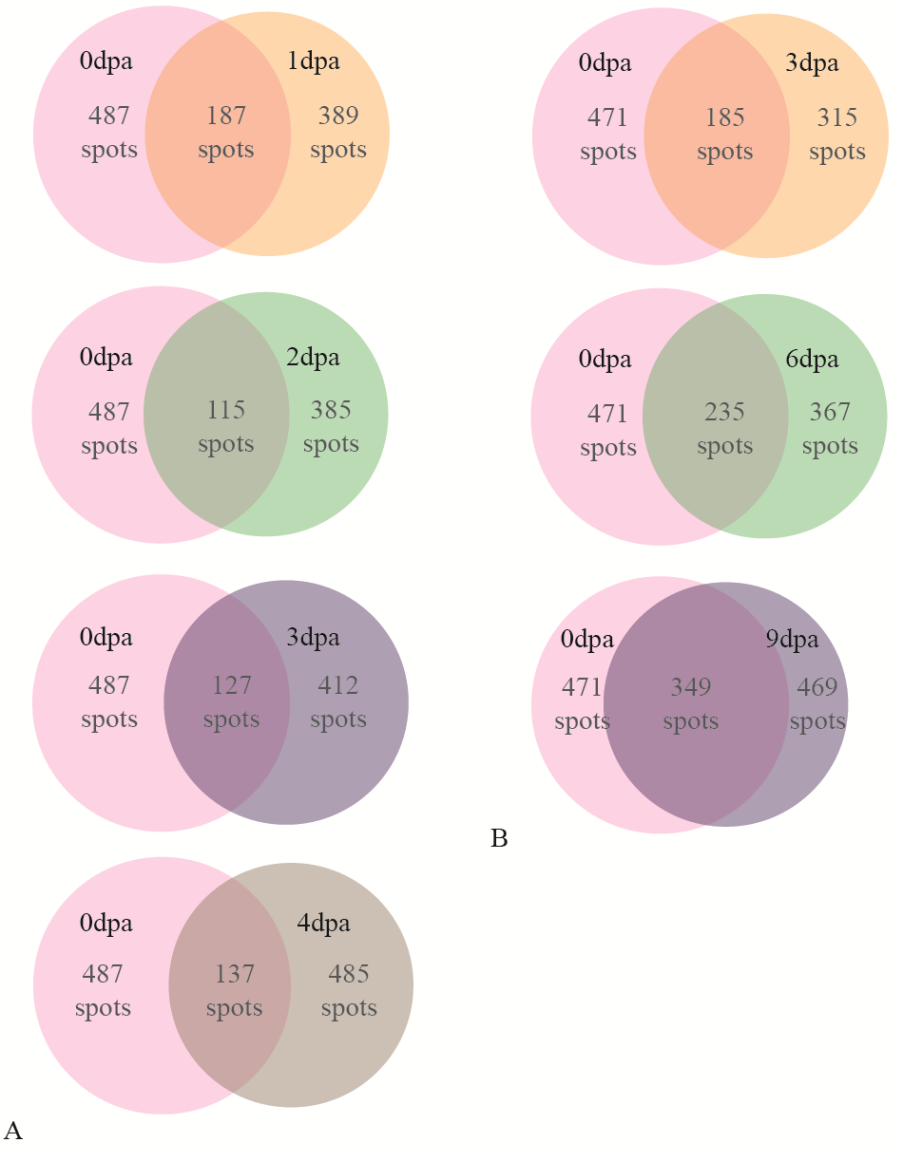

Figure 5: Venn diagram constructed from the data obtained after analysing the gels in PDQuest software version 8.0. A) depicts the number of spots which are commonly present in the wound healing stages of tail when compared to the resting tail. B) depicts the number of spots which are commonly present in the wound healing stages of limb when compared to the resting limb.

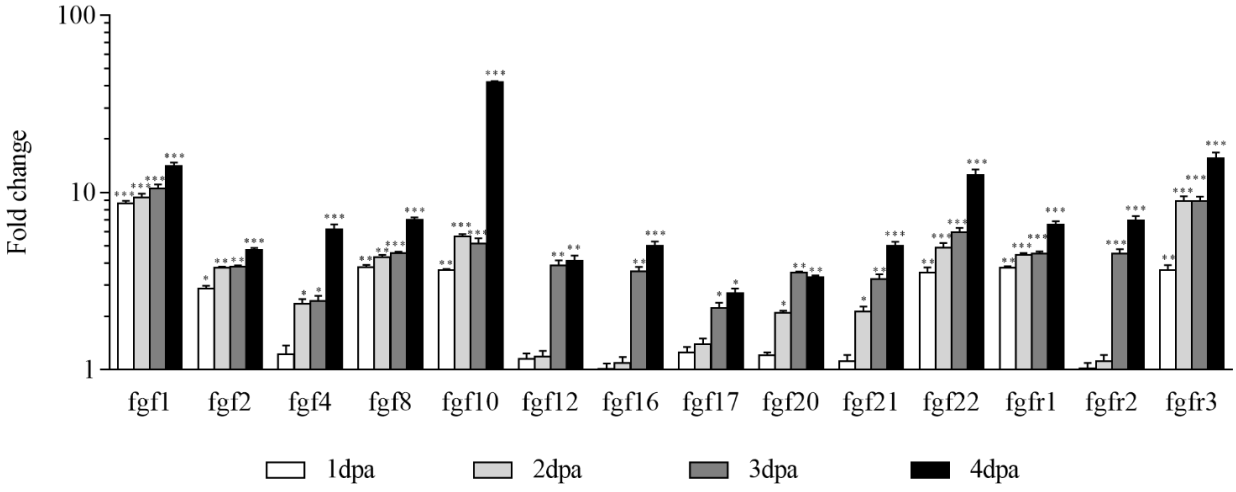

Figure 6A: Relative transcript level expression of fgfs in tail wound healing stages. Fold change values for time points was normalized with that of the resting stage of tail. Error bars represent standard error of mean and asterisk represent p value where * represents p≤0.05, ** stands for p≤0.01 and *** depicts p≤0.001, (n=6)

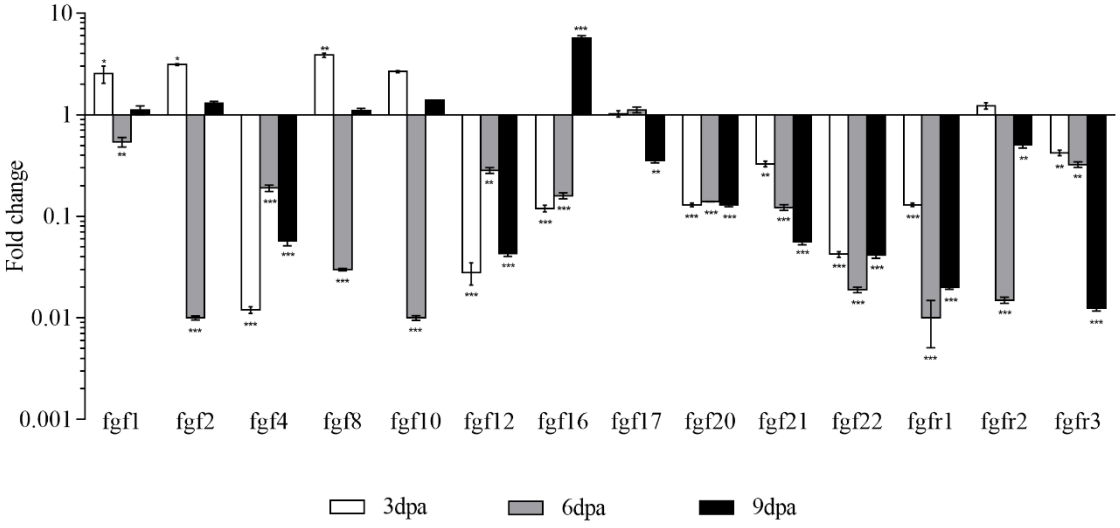

Figure 6B: Relative transcript level expression of fgfs during limb wound healing. Fold change values for time points was normalized by those of the resting stage of limb. Error bars represent standard error of mean and asterisk represent p value where * represents p≤0.05, ** stands for p≤0.01 and *** depicts p≤0.001, (n=6);

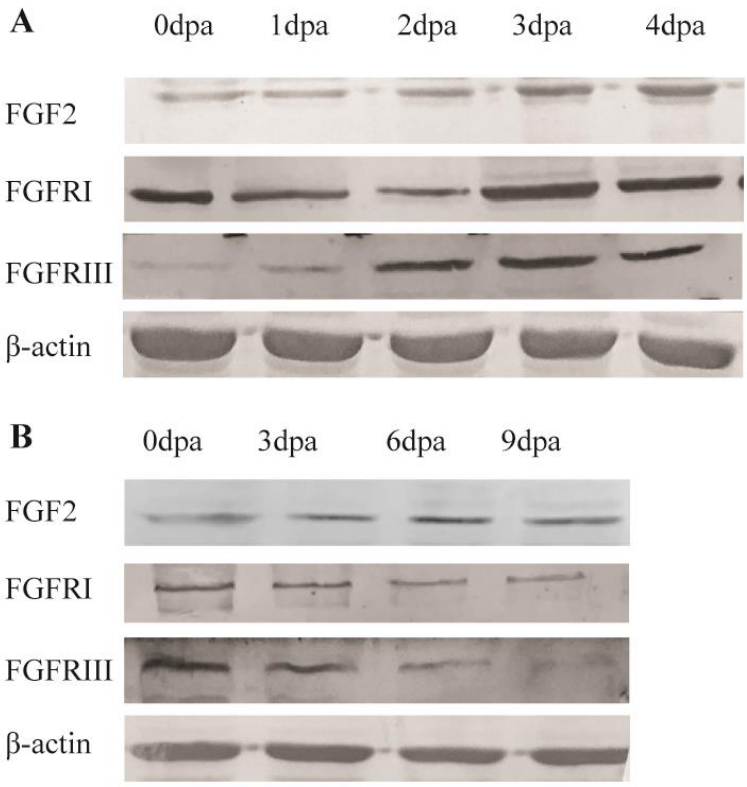

Figure 7: Western blot of tail limb wound healing stages. A) represents western blot images of FGF2, FGFRI and FGFRIII for tail on 0dpa, 1dpa, 2dpa, 3dpa and 4dpa; B) represents western blot images of FGF2, FGFRI and FGFRIII for limb on 0dpa, 3dpa, 6dpa and 9dpa

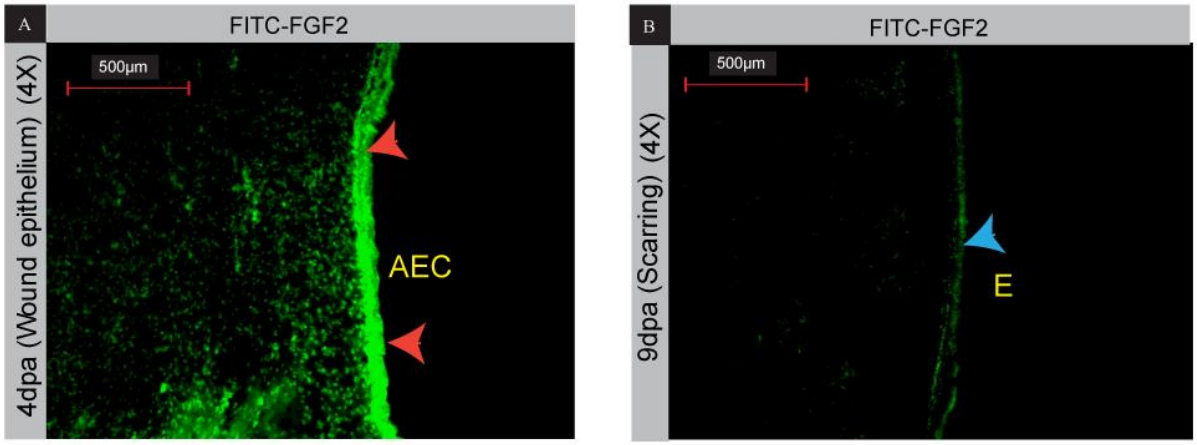

Figure 8: FGF2 localization in tail epithelium and scarred limb. A) indicates FGF2 localization in the AEC of tail at wound epithelium stage (orange arrowhead) and B) indicates faint localization signals of FGF2 in the limb healing stage (blue arrowhead).

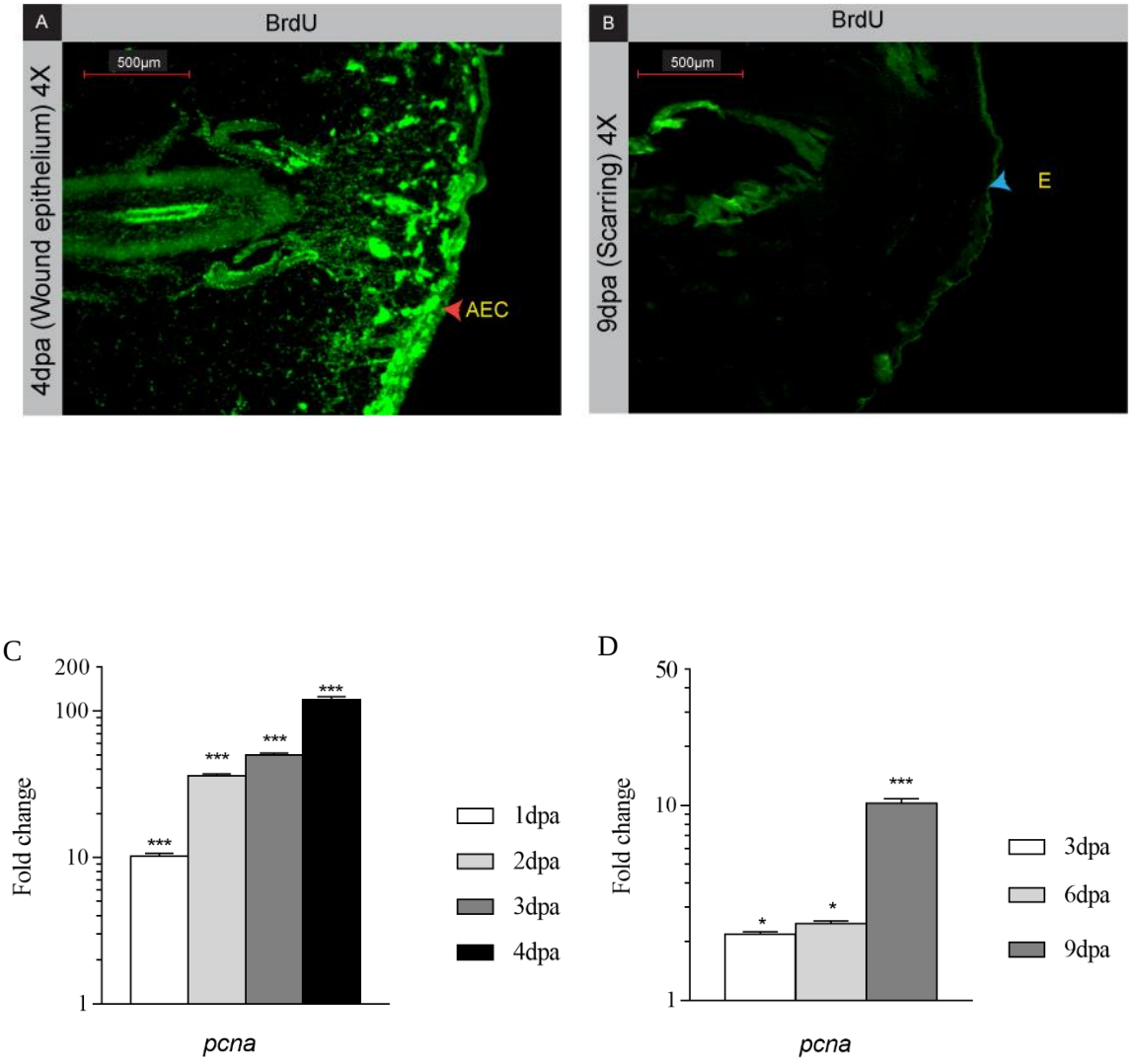

Figure 9: BrdU staining for studying proliferation A) and B) are the images for tail at 4dpa and limb at 9dpa showing BrdU incorporation wherein orange arrowhead shows the BrdU labelling in AEC and blue arrowhead represents the epithelium which is minimally representing BrdU in limb. C) Relative transcript level expression of *fgfs* and *pcna* in tail wound healing. Fold change values for time points was normalized with that of the resting stage of tail. D) Relative transcript level expression of fgfs and *pcna* during limb wound healing. Fold change values for time points was normalized by those of the resting stage of limb. Error bars represent standard error of mean and asterisk represent p value where * represents $p \leq 0.05$, and *** depicts $p \leq 0.001$, (n=6).

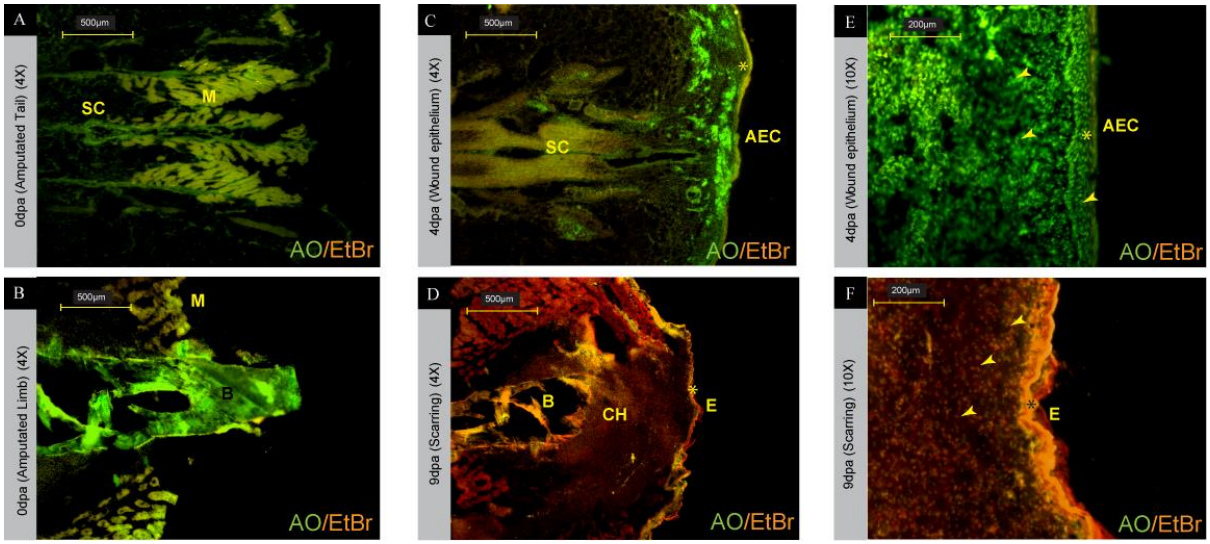
A
0dpa (Amputated Tail) (4X)
500µm
SC
M
AO/EtBr
C
4dpa (Wound epithelium) (4X)
500µm
SC
AEC
AO/EtBr
E
4dpa (Wound epithelium) (10X)
200µm
AEC
AO/EtBr
B
0dpa (Amputated Limb) (4X)
500µm
M
B
AO/EtBr
D
9dpa (Scarring) (4X)
500µm
B
CH
E
AO/EtBr
F
9dpa (Scarring) (10X)
200µm
E
AO/EtBr

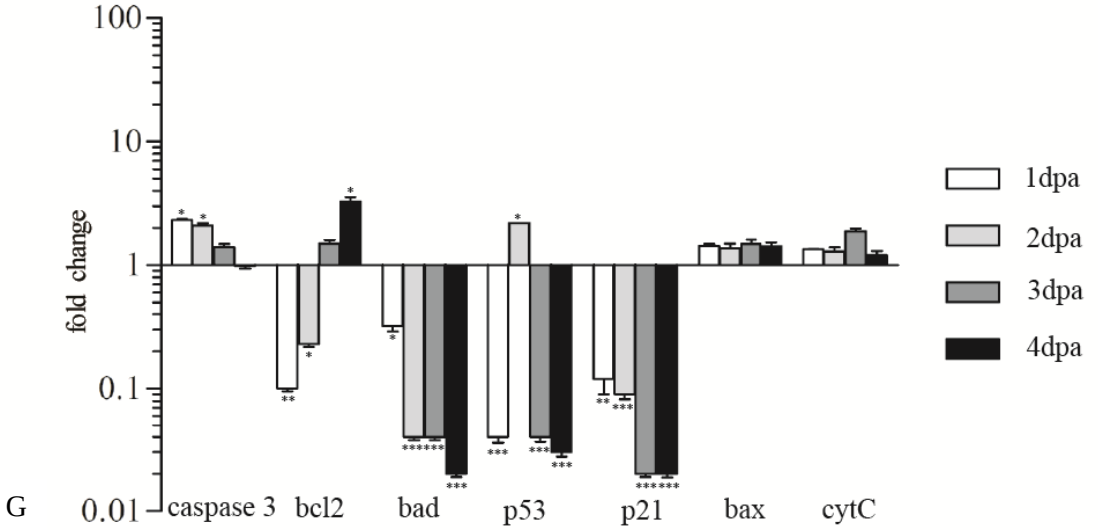
G
fold change
100
10
1
0.1
0.01
caspase 3
bcl2
bad
p53
p21
bax
cytC
1dpa
2dpa
3dpa
4dpa

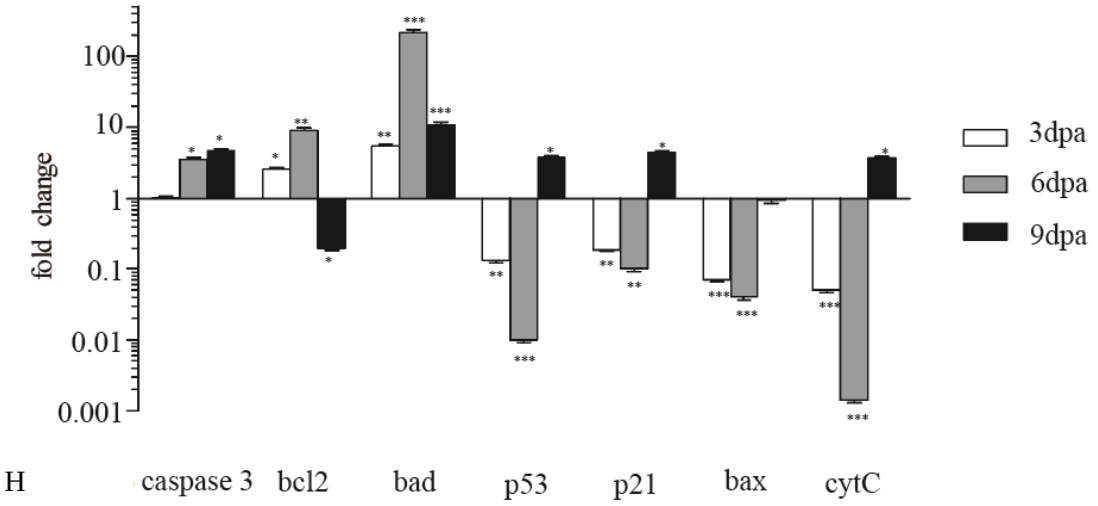
H
fold change
100
10
1
0.1
0.01
0.001
caspase 3
bcl2
bad
p53
p21
bax
cytC
3dpa
6dpa
9dpa

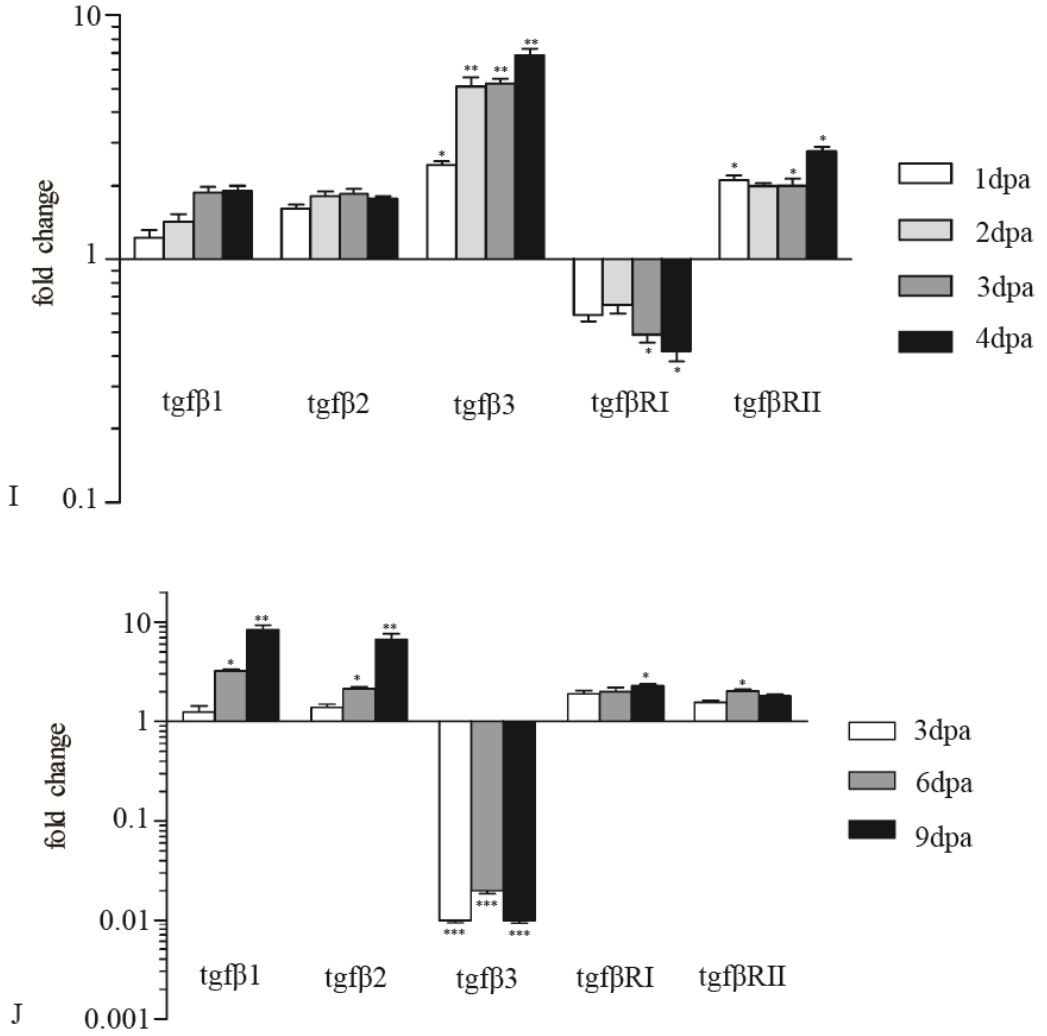

Figure 10: Represents Acridine orange and ethidium bromide staining wherein A) and B) are the tail and limb post-amputation while C) and D) are the wound healing stages for tail and limb and their higher magnified images are E) and F). The arrow heads in figure E) denotes. the live cells which are visible due to green fluorescence whereas arrow head in figure F) depicts the pro and apoptotic cells which are orange and red in color respectively. "*" represents the area which is depicted in the magnified image. (AEC: apical epithelial cap, B: bone, CH: chondrocytes E: epithelium, M: Muscle, SC: spinal cord,). G) Relative transcript level expression of apoptotic markers during wound healing in tail. Fold change values for time points was normalized with those of the resting stage of tail. H) Relative transcript level expression of apoptotic markers during wound healing in the limb; I) and J) denote fold change values of tgf-β in tail and limb wound healing stages Fold change values for time points was normalized with those of the resting stage of limb. Error bars represent standard error of mean and asterisk indicates p value where * shows $p \leq 0.05$, ** depicts $p \leq 0.01$ and *** stands for $p \leq 0.001$.

DISCUSSION:

Lizards are amniote model of regeneration having the maximum evolutionary proximity to the mammals. Hence, there are similarities between the embryonic stages of reptiles and mammals (Lozito *et al.*, 2016). However, lizards are capable of post-embryonic development, *viz.*, regeneration of the lost tail, which is lacked by their mammalian counterparts. Interestingly, lizards can restore only their tail but no other appendage via epimorphic regeneration (McLean and Vickaryous, 2011). Nonetheless, in order to facilitate regeneration in the tail, it needs to heal without the formation of a scar and hence, is called as scar-free wound healing. On the contrary, the amputated limb heals with a scar. Herein, an attempt was made to compare the differences in the mechanisms underlying scar-free and scarred wound healing in lizard.

In order to study the mechanisms underlying scar-free and scarred wound healing, 2-Dimensional gel electrophoresis technique was performed for all the stages. On analysis we obtained a number of proteins which were differentially expressed across the wound healing stages. Many growth factors were identified from 2DGE and different fgfs were also found amongst them. Very few fgfs have a defined role in the process of regeneration as well as in the scarred wound healing process. Hence this pathway was targeted for the study. Before going into the molecular mechanism of healing, a histology profile was generated.

In scar-free wound healing, the histology of healing tail reveals a proliferating epidermis which at 2dpa was 44.65µm thick and was measured to be of a thickness 91.93µm during the wound epithelium stage i.e. at 4dpa stage. It is noticeable that the epidermis is continuously proliferating at the wound site as its thickness in the normal intact skin is only 12.52µm. Similar results were observed by McLean and Vickaryous (2011) wherein the *Eublepharis* lizard shows a newly formed wound epithelium that continues to proliferate and thicken (up to 12 cell layers thick compared to 4-7 in the original epidermis), especially at the apical epithelial cap. In other regeneration models (e.g. urodeles, teleosts) the AEC has a well-documented role, as a source of morphogenetic information quite comparable to the apical ectodermal ridge of developing limb (Dinsmore *et al.*, 1997; Poss *et al.*, 2004). However, it is now accepted that under no circumstances formation of AEC happens in case of an amputated limb. Further, it has been documented that on amputation of a limb, the blood vessels rupture and the loss of blood is more as compared to that of the tail wherein the bleeding is kept at minimum due to contraction of precapillary sphincters (Delrome *et al.*, 2012). Moreover, because of the prolonged bleeding in limb, a thick blood clot forms at the site of injury. Not surprisingly, on 3dpa it was observed that the cut surface of the limb was covered only by a scab with no epithelial lining underneath

as against the autotomy surface of tail wherein the epithelial covering was observed as early as on 1dpa. However, on completion of wound closure at 9dpa, a thick scar tissue of 200µm covers the cut surface of limb and the overlying epidermis at this point is just 17µm thickness, same as what used to be in a resting epithelial layer of limb, suggesting that AEC is not formed in limb and instead scarred stump is formed.

After achieving the histology profile, fgf family ligands were screened for their expression in tail and limb wound healing stages. A steady increase in the mRNA levels of *fgf1*, *fgf2*, *fgf8*, and *fgf12, fgf16, fgf17, fgf20, fgf21* and *fgf22* was observed in regenerating tail as healing progressed from 0 dpa to 4 dpa. However, when the expression levels in all the stages were compared to that of resting stage, i.e., 0dpa, a sharp increase of 50-fold change was noticed for *fgf10* on 3dpa unlike the other fgfs screened. In tandem with the rise in *fgfs*, *fgfr1*, *fgfr2* and *fgfr3* were also found elevated from 1dpa to 4dpa. However, the limb healing stages which are 0, 3, 6 and 9dpa showed a different trend to that observed in the tail. There was an increase in transcripts of *fgf1, fgf2, fgf8* and *fgf10* at 3dpa but a sharp decline was seen in subsequent stages. *fgf4, fgf12, fgf20, fgf21, fgf22* were down-regulated till 9dpa which also coincided with the levels of receptor *fgfr1, fgfr2* and *fgfr3*. However, *fgf16* after 3dpa shot up at 6dpa and then was subdued in next 3days. The role of fgfs has been discussed below in detail.

It has been well authenticated that the wound epithelium stratifies to form AEC through regulated cell division under the influence of various putative paracrine factors (Grose *et al*., 2002; Mesher *et al*., 2004). An up-regulation in fgfs was observed, in all the time points studied, in the autotomized tail till the wound epithelium formation was accomplished at 4dpa. *fgf1* and *fgf2* transcripts were significantly higher in the healing tail and so was the FGF2 protein level, than in the resting one. Alibardi (2012) in one of his studies observed positive immunolocalization for FGF2 in the epidermis of lizard tail which accords with our findings wherein FGF2 was localized in the AEC and the underlying tissue, however limb showed positive staining only in the epithelium at the wound site suggesting a barrier formation between epithelium and underlying tissue which does not allow the cells to undergo proliferation. FGF2 and FGF1 are required for the epidermis to proliferate and form the AEC (Han *et al*., 2005; Alibardi *et al*., 2010; Yadav *et al*., 2012; Pillai *et al*., 2013). The same trend has been reported in chick limb development as well (Ornitz *et al*., 2016), but in case of lizard limb healing, it was observed that these factors are either absent or their levels are too low to facilitate re-growth. FGF8 has a known role in the outgrowth of the limb of chick wherein it translocates from the epidermis to the underlying mesenchymal cells (Han *et al*., 2001). In

lizard tail a steady increase of FGF8 was seen from 1dpa to 4dpa suggesting that its outgrowth must be very similar to that of the limb in a developing chick embryo. On the contrary, in the lizard limb, the absence of FGF8 may lead to stalling of outgrowth as well. In order to induce expression of FGF8, FGF10 is a prerequisite and there are ample evidences suggesting that FGF10 induces FGF8 in the ectoderm and Shh in mesoderm, proposing FGF10 to be an endogenous mesenchymal factor playing a pivotal role in initial budding and outgrowth of the vertebrate limb (Ohuchi *et al*., 1997; Xu *et al*., 1998; Ornitz *et al*., 2016). The evidences mentioned above justifies the results in tail wound healing, wherein an increase in transcript level of *fgf10* along with *fgf8* was observed. The lack of *fgf8* and *fgf10* in lizard's limb would be playing a crucial role in the formation of the scarred stump at the amputated end. An increase in fgf8 and fgf10 leads to proliferation which was clearly seen in the western of tail healing stages wherein a constant increase in PCNA was documented. Limb healing stages did show some increase in the protein levels of PCNA though not comparable to the tail, also their appearance was at a much later stage which might be due to collagen proliferation and deposition. To support this hypothesis, BrdU was incorporated in both tail and limb during healing and the images clearly portray that BrdU gets accumulated in the AEC and the mesenchymal cells underlying it in tail while in limb BrdU is seen only in the epithelium and the collagen deposited under it. Further evidences for proliferation and apoptosis were gathered from acridine orange and ethidium bromide stained tissue sections. The tail tissue at wound epithelium stage (4dpa) were predominated by green colored proliferating cells. On the contrary, a corresponding stage in limb (9dpa) revealed largely pro-apoptotic (yellow) and apoptotic (red) cells, indicating high apoptosis ensuing during the scar formation. Apart from these FGFs mentioned above, another major one required for sustaining the epidermis is FGF20 (Whitehead *et al*., 2005). FGF20 gets triggered by Wnt/β-catenin which in turn is regulated by ROS production. In *Xenopus* tadpole tail regeneration, higher levels of FGF20 were detected in the regenerating tissue when compared to the resting tissue (Love *et al*., 2013). In this study, tail which undergoes scar-free healing showed an increase in *fgf20* but the same was down-regulated in limb again implying that the limb has an alternate path of healing which in due course leads to scarring.

Scarring is normally seen in mammalian injury, and limb healing in lizard also follows similar mechanism. The major growth factor that has a known role in scarring is the TGFβ (Klass *et al*., 2009; Kristi *et al*., 2017). One of the studies performed on human fetal skin revealed that if TGFβ1 and TGFβ2 cause scarring whereas in another study done on rat skin shows if

expression of TGFβ3 in increased, the scarring reduces considerably (Soo *et al*., 2003; Larson *et al*., 2010). This leads to an inference, that TGFβ1 and TGFβ2 have a well-defined role in fibronectin deposition which was also observed during limb healing stages. In the light of the above discussion it could be presumed that for scar-less wound healing, deposition of fibronectin is avoided and hence *tgfβ3* was found to be elevated during tail wound healing stages. Not only does TGFβ have a role in fibrosis but it also plays a major role in inducing apoptosis (Perlman *et al*., 2001; Li *et al*., 2002). Lafon and coworkers found out that TGFβ1 induces apoptosis through c-fos and c-jun genes in human ovarian cancer cells (Lafon *et al*., 1996). In the current study both TGFβ induced and p53 mediated apoptosis was studied for all the stages of healing in tail as well as limb. In tail, initially a 2-fold increase in *caspase 3* and *p53* was observed at 1dpa and 2dpa, however, these levels drop at 3dpa and 4dpa which also can be seen in the Cleaved Caspase-3 immunoblot. In order to keep the tail growing, proliferation has to surpass apoptosis which was observed in this study wherein *p53, p21, bad, bax* and even the TGFβs were down-regulated. Limb healing showed higher levels of p53 and p21 only at 9dpa but a 200-fold surge was noted in bad expression at 6dpa. This is because in scarred wound healing at granulation phase it is observed that the myofibroblasts disappear, leaving behind the scar (Desmouliere *et al*., 1995). Apoptosis is a prerequisite for the entire mechanism and thus higher levels of bad at 6dpa are justified.

Other studies carried out in lizard tail and limb healing are focused on specific stages of regeneration like wound healing and blastema in tail and scarring in limb. For instance, a study by Vitulo *et al*., 2017 in *Podarcis muralis* analyses the transcriptomic expression during tail and limb healing but specifically at the wound healing and blastema stages. The study did recognize wnt and fgfs for playing major roles in blastema recruitment which ultimately leads to regeneration of tail and failure of limb formation. Another study by Alibardi *et al*., 2010 in *Podarcis sicula* reveals that cell proliferation is reduced in limb healing as compared to tail, an observation which coincides with the present study. Nevertheless, the results presented in the current work are based on a temporal expression pattern of some of the key molecules which are required to regulate various cellular events that facilitate the successful realization of the major milestones in the process of wound healing which has not yet been carried out in any of the lizard models. Through this study it can be construed that the central events like proliferation, apoptosis and angiogenesis do occur in both scar-free as well as in scarred wound healing, but the duration for which they last and the point at which these are patterned, differs

and this difference causes the tail to follow scar free healing, while the limb undergoes the scarred wound healing process.

CONCLUSION:

Epimorphic regeneration being a postembryonic developmental process involves certain characteristic cellular and molecular processes like inflammation, cell proliferation, migration, apoptosis as well as re-patterning. Scarred wound healing also involves similar processes but the duration and sequence of events is altered from that of scar-free wound healing. An attempt was made to obtain stage specific protein profile of wound healing in tail and limb of *Hemidactylus flaviviridis* using two-dimensional gel electrophoresis. 2DGE revealed many growth factors which are necessary for carrying out the process of regeneration as well as in scarring. FGFs were found to be differentially expressed across the stages of wound healing in tail and limb and hence fgf family ligands were screened for the first time in lizards tail and limb wound healing stages. Lizards achieve the wound epithelium stage at 4dpa whereas the limb requires 9dpa for full wound closure. Various processes and signalling molecules play an important role in deciding the course of healing. In this study, it was observed that proliferation of epidermal cells and the mesenchymal cells is triggered as soon as the there is an injury to the tail, however the limb shows proliferation only of the fibroblast cells at a later stage of healing. Various fgf genes were up-regulated in order to form the proliferating epidermis which eventually forms AEC at 4dpa in tail. The proliferation of epidermal cells follows the activation of PI3K-Akt signalling pathway as their levels were found to be elevated along with fgfs. Instead of proliferation at an early stage, limb showed apoptosis to be persistent for a longer duration wherein the expression of bad and caspase 3 were seen at an early stage at 3dpa and caspase remained high till later stage along with p53 and p21 which is triggered by the p38-MAPK pathway as evident from the result. Apoptosis was apparent at 1dpa in tail but it was subsequently found to be down-regulated. Apart from fgfs, tgf-β members are also a pre-requisite in wound healing and the results suggest that tgf-β1 and tgf-β2 are involved in the scarring and apoptosis as their levels were significantly high in the stages of limb wound healing. In contrast to this, tgf-β3 promotes scar-free wound healing which accorded with the results obtained from the tail wound healing stages.

Even though all processes occur in both the wound healing, their occurrence and duration are quite different which may be the reason which allows the tail to heal in scar-free manner and

regain it completely whereas the limb undergoes scarred wound healing which ultimately forms a stump with no functionality.

PAPERS PUBLISHED:

1. Murawala H, Ranadive I, Patel S, Desai I, Balakrishnan S. Protein expression pattern and analysis of differentially expressed peptides during various stages of tail regeneration in Hemidactylus flaviviridis. *Mechanisms of development*. 2018 Apr 1;150:1-9.

2. Buch PR, Ranadive I, Desai I & Balakrishnan S. Cyclooxygenase-2 interacts with MMP and FGF pathways to promote epimorphic regeneration in lizard Hemidactylus flaviviridis. *Growth Factors*. July 2018
   DOI:10.1080/08977194.2018.1497021)

3. Ranadive I, Patel S, Buch PR, Uggini GK, Desai I, Balakrishnan. Inherent variations in the cellular events at the site of amputation orchestrate scar-free wound healing in the tail and scarred wound healing in the limb of lizard Hemidactylus flaviviridis. *Wound Repair and Regeneration*. July 2018
   DOI:10.1111/wrr.12659

REFERENCE:

1. Alibardi L. Ultrastructural features of the process of wound healing after tail and limb amputation in lizard. *Acta Zoologica*. 2010 Jul 1;91(3):306-18.
2. Alibardi L, Lovicu FJ. Immunolocalization of FGF1 and FGF2 in the regenerating tail of the lizard Lampropholis guichenoti: implications for FGFs as trophic factors in lizard tail regeneration. *Acta histochemica*. 2010 Sep 1;112(5):459-73.
3. Alibardi L. Observations on FGF immunoreactivity in the regenerating tail blastema, and in the limb and tail scars of lizard suggest that FGFs are required for regeneration. *Belgian Journal of Zoology*. 2012 Jan 1;142(1).
4. Barrientos S, Stojadinovic O, Golinko MS, Brem H, Tomic-Canic M. Growth factors and cytokines in wound healing. *Wound repair and regeneration*. 2008 Sep 1;16(5):585-601.
5. Bradford MM. A rapid and sensitive method for the quantitation of microgram quantities of protein utilizing the principle of protein-dye binding. *Analytical biochemistry*. 1976 May 7;72(1-2):248-54.
6. Brockes JP, Kumar A, Velloso CP. Regeneration as an evolutionary variable. *The Journal of Anatomy*. 2001 Aug;199(1-2):3-11.
7. Buch PR, Sarkate P, Uggini GK, Desai I, Balakrishnan S. Inhibition of Cyclooxygenase-2 Alters Wnt/β-Catenin Signaling in the Regenerating Tail of Lizard Hemidactylus flaviviridis. *Tissue Engineering and Regenerative Medicine*. 2017 Apr 1;14(2):171-8.
8. Carlson B M. Chapter 05 - Tissue Interactions in Regeneration, 2007 (1970), 93–109.
9. del Moral PM, De Langhe SP, Sala FG, Veltmaat JM, Tefft D, Wang K, Warburton D, Bellusci S. Differential role of FGF9 on epithelium and mesenchyme in mouse embryonic lung. *Developmental biology*. 2006 May 1;293(1):77-89.
10. Delorme SL, Lungu IM, Vickaryous MK. Scar-free wound healing and regeneration following tail loss in the leopard gecko, Eublepharis macularius. *The Anatomical Record*. 2012 Oct 1;295(10):1575-95.
11. Desmouliere A, Redard M, Darby I, Gabbiani G. Apoptosis mediates the decrease in cellularity during the transition between granulation tissue and scar. *The American journal of pathology*. 1995 Jan;146(1):56.
12. Dinsmore CE. Tail regeneration in the plethodontid salamander, Plethodon cinereus: Induced autotomy versus surgical amputation. *Journal of Experimental Zoology* Part A: Ecological Genetics and Physiology. 1977 Feb 1;199(2):163-75.
13. Enoch S, Harding K. Wound bed preparation: the science behind the removal of barriers to

healing. *Wounds*. 2003 Jul;15(7):213-29.

14. Gilbert SF. *Developmental Biology* (10th Ed.). Sunderland, MA: Sinauer Associates 2014.
15. Gillitzer R, Goebeler M. Chemokines in cutaneous wound healing. *Journal of leukocyte biology*. 2001 Apr 1;69(4):513-21.
16. Grose R, Werner S, Kessler D, Tuckermann J, Huggel K, Durka S, Reichardt HM, Werner S. A role for endogenous glucocorticoids in wound repair. *EMBO reports*. 2002 Jun 1;3(6):575-82.
17. Han M, Yang X, Taylor G, Burdsal CA, Anderson RA, Muneoka K. Limb regeneration in higher vertebrates: developing a roadmap. *The Anatomical Record*. 2005 Nov 1;287(1):14-24.
18. Hughes RN. Functional biology of clonal animals. *Springer Science & Business Media*; 1989 Oct 31.
19. Kiritsi D, Nyström A. The role of TGFβ in wound healing pathologies. *Mechanisms of ageing and development*. 2017 Nov 11.
20. Klass BR, Grobbelaar AO, Rolfe KJ. Transforming growth factor β1 signalling, wound healing and repair: a multifunctional cytokine with clinical implications for wound repair, a delicate balance. *Postgraduate Medical Journal*. 2009 Jan 1;85(999):9-14.
21. Lafon C, Mathieu C, Guerrin M, Pierre O, Vidal S, Valette A. Transforming growth factor beta 1-induced apoptosis in human ovarian carcinoma cells: protection by the antioxidant N-acetylcysteine and bcl-2. *Cell growth & differentiation*: the molecular biology journal of the American Association for Cancer Research. 1996 Aug;7(8):1095-104.
22. Larson BJ, Longaker MT, Lorenz HP. Scarless fetal wound healing: a basic science review. *Plastic and reconstructive surgery*. 2010 Oct;126(4):1172.
23. Li Y, Liu Y, Fu Y, Wei T, Le Guyader L, Gao G, Liu RS, Chang YZ, Chen C. The triggering of apoptosis in macrophages by pristine graphene through the MAPK and TGF-beta signaling pathways. *Biomaterials*. 2012 Jan 1;33(2):402-11.
24. Livak KJ, Schmittgen TD. Analysis of relative gene expression data using real-time quantitative PCR and the $2^{-\Delta\Delta CT}$ method. *Methods*. 2001 Dec 1;25(4):402-8.
25. Love NR, Chen Y, Ishibashi S, Kritsiligkou P, Lea R, Koh Y, Gallop JL, Dorey K, Amaya E. Amputation-induced reactive oxygen species are required for successful Xenopus tadpole tail regeneration. *Nature cell biology*. 2013 Feb;15(2):222
26. Madala SK, Pesce JT, Ramalingam TR, Wilson MS, Minnicozzi S, Cheever AW, Thompson RW, Mentink-Kane MM, Wynn TA. Matrix metalloproteinase 12-deficiency augments

extracellular matrix degrading metalloproteinases and attenuates IL-13–dependent fibrosis. *The Journal of Immunology*. 2010 Apr 1;184(7):3955-63.

27. Makanae A, Mitogawa K, Satoh A. Cooperative inputs of Bmp and Fgf signaling induce tail regeneration in urodele amphibians. *Developmental biology*. 2016 Feb 1;410(1):45-55.
28. Matsumoto K, Ema M. Roles of VEGF-A signalling in development, regeneration, and tumours. *The Journal of Biochemistry*. 2014 May 16;156(1):1-0.
29. McLean KE, Vickaryous MK. A novel amniote model of epimorphic regeneration: the leopard gecko, Eublepharis macularius. *BMC developmental biology*. 2011 Dec;11(1):50.
30. Murawala H, Ranadive I, Patel S, Desai I, Balakrishnan S. Protein expression pattern and analysis of differentially expressed peptides during various stages of tail regeneration in Hemidactylus flaviviridis. *Mechanisms of development*. 2018 Apr 1; 150:1-9.
31. Mutsaers SE, Bishop JE, McGrouther G, Laurent GJ. Mechanisms of tissue repair: from wound healing to fibrosis. *The international journal of biochemistry & cell biology*. 1997 Jan 1;29(1):5-17.
32. Ohuchi H, Nakagawa T, Yamamoto A, Araga A, Ohata T, Ishimaru Y, Yoshioka H, Kuwana T, Nohno T, Yamasaki M, Itoh N. The mesenchymal factor, FGF10, initiates and maintains the outgrowth of the chick limb bud through interaction with FGF8, an apical ectodermal factor. *Development.* 1997 Jun 1;124(11):2235-44.
33. Ollendorff V, Planche J, Ott MO, Pizette S, Coulier F, Birnbaum D. Expression of the Fgf6 gene is restricted to developing skeletal muscle in the mouse embryo. *Development.* 1993 Jun 1;118(2):601-11.
34. Ornitz DM, Itoh N. An Introduction to the Fibroblast Growth Factors. *Fibroblast Growth Factors: Biology And Clinical Application-Fgf Biology And Therapeutics*. 2016 Dec 27:1.
35. Penn JW, Grobbelaar AO, Rolfe KJ. The role of the TGF-β family in wound healing, burns and scarring: a review. *International journal of burns and trauma*. 2012;2(1):18.
36. Perlman R, Schiemann WP, Brooks MW, Lodish HF, Weinberg RA. TGF-β-induced apoptosis is mediated by the adapter protein Daxx that facilitates JNK activation. *Nature cell biology*. 2001 Aug;3(8):708.
37. Pillai A, Desai I, Balakrishnan S. Pharmacological inhibition of FGFR1 signaling attenuates the progression of tail regeneration in the northern house gecko Hemidactylus flaviviridis. *International journal of life sciences biotechnology and pharma research*. 2013;2:263-78.
38. Poss KD, Keating MT, Nechiporuk A. Tales of regeneration in zebrafish. *Developmental Dynamics*. 2003 Feb 1;226(2):202-10.
39. Sanchez Alvarado A. Regeneration in the metazoans: why does it happen. *Bioessays.*

2000;22(6):578590.

40. Sonnemann KJ, Bement WM. Wound repair: toward understanding and integration of single-cell and multicellular wound responses. *Annual review of cell and developmental biology*. 2011 Nov 10;27:237-63.
41. Soo C, Beanes SR, Hu FY, Zhang X, Dang C, Chang G, Wang Y, Nishimura I, Freymiller E, Longaker MT, Lorenz HP. Ontogenetic transition in fetal wound transforming growth factor-β regulation correlates with collagen organization. *The American journal of pathology*. 2003 Dec 1;163(6):2459-76.
42. Vitulo N, Dalla Valle L, Skobo T, Valle G, Alibardi L. Transcriptome analysis of the regenerating tail vs. the scarring limb in lizard reveals pathways leading to successful vs. unsuccessful organ regeneration in amniotes. *Developmental Dynamics*. 2017 Feb 1;246(2):116-34.
43. Whitehead GG, Makino S, Lien CL, Keating MT. fgf20 is essential for initiating zebrafish fin regeneration. *Science*. 2005 Dec 23;310(5756):1957-60.
44. Xu X, Weinstein M, Li C, Naski M, Cohen RI, Ornitz DM, Leder P, Deng C. Fibroblast growth factor receptor 2 (FGFR2)-mediated reciprocal regulation loop between FGF8 and FGF10 is essential for limb induction. *Development*. 1998 Feb 15;125(4):753-65
45. Yadav M, Anusree P, Desai I, Suresh B. Influence of extraneous FGF-2 and its antagonist anti-FGF-2 on the progress of tail regeneration in Hemidactylus flaviviridis. *Indian journal of fundamental and applied life sciences*. 2012 Apr;2(2):164-72.

Isha Ranadive
(Ph.D. Student)

Prof. B. Suresh
(Ph.D. Supervisor)